Preprints of the 19th World Congress
The International Federation of Automatic Control
Cape Town, South Africa. August 24-29, 2014

PD-Super-Twisting Second Order Sliding Mode Tracking Control for a Nonholonomic Wheeled Mobile Robot

Ebrahim Samer El youssef * **Nardênio Almeida Martins** **
Edson Roberto De Pieri * **Ubirajara Franco Moreno** *

* *Universidade Federal de Santa Catarina, Florianópolis, SC 88040-900 BRAZIL (e-mail: ebrahim@ boulder.nist.gov).*
** *Universidade Estadual de Maringá, Maringá, PR 87020-900 BRAZIL (e-mail: nardenio@din.uem.br, namartin@din.uem.br)*

Abstract: A robust solution to the trajectory tracking control problem for a nonholonomic wheeled mobile robot should deal with the existence of structural and parameter uncertainties, external disturbances and operating limitations. The first order sliding control with boundary layer is a common and suitable solution that can ensure chattering attenuation, but with poor degree of robustness. Fortunately, higher order sliding mode control can achieves greater degree of robustness with the reduction of the chattering phenomenon. Based on this knowledge, a control strategy is proposed using a super-twisting sliding mode control, which enforces a second order sliding mode, in cascade with an inverse dynamic control with proportional plus derivative control to solve the problem achieving good robustness. This linear control technique plays an important role in increasing the robustness by mitigating the influence of neglected dynamics. Experimental results are explored to show the effectiveness of the proposed strategy.

1. INTRODUCTION

Although a *nonholonomic* wheeled mobile robots (WMR) has movement constraints it regards advantages of less weight and good energy efficiency and is useful in many applications [Siciliano and Khatib, 2008]. A typical example of this kind of system is a differential wheeled mobile robot (DWMR) [Yang and Kim, 1999, Chwa, 2004, Ferrara and Rubagotti, 2008, Park et al., 2009], which comprises a body supported by two free wheels and two simple wheels actuated by DC motors.

An important control problem for the autonomous robot locomotion is the tracking of a given feasible trajectory parameterized in time with robustness despite of parametric and structural uncertainties, disturbances and system limitations. Some solutions for this problem have been addressed by means of sliding mode control (SMC) technique due to its good performance and robustness. Yang and Kim [1999] and Chwa [2004] proposed an inverse dynamic control combined with a FOSMC with BL to achieve a solution with chattering phenomenon reduction for a DWMR. The inverse dynamic control compensates known forces and torques and FOSMC with BL ensures that trajectories are tracked.

Unfortunately, there is a robustness reduction as a consequence of employing the BL technique that relax the sliding constraints to mitigate chattering in closed loop with FOSMC. This phenomenon consists of oscillations with limited amplitude and frequency on the system states that occurs when there are (i) neglected dynamics excited by the high frequency discontinuous switching control signal or (ii) switching frequency limitation. Yang and Kim [1999] explored experimental results that have led to high errors relative to the size of the robot due to neglected dynamics. In sequence Chwa [2004] explored just simulation with perfect compensation of the system dynamics, so escaping the elements that causes chattering. In their work, Park et al. [2009] applies a similar control structure, but using an additional neural network control to compensate uncertainties in the dynamics. No discussion about practical problems in terms of experiments are presented with results limited to simulations, therefore, dismissing the robustness that a SMC should provide for the closed-loop system and the chattering problems.

The fact is that BL as others solutions associated with FOSMC can imply in a disadvantageous trade-off between robustness and chattering reduction [Utkin et al., 2009]. Some better solutions have been developed by means of a second order sliding mode (SOSMC) application, that provides continuous control signals with discontinuous derivative capable of enforcing the sliding mode constraints and achieving robustness [Levant, 1993, Fridman and Levant, 2002]. An important result was provide by Levant [1993], that showed that if there is an imperfection in the switching control due to system limitations, than higher order sliding mode is more effective in terms of robustness.

Therefore, in this paper a control strategy based on the super-twisting sliding mode control (STSMC), a SOSMC technique that has good numeric performance and do not depend on the time derivative of $\sigma(x)$ [Levant, 1993, Fridman and Levant, 2002] is proposed to solve the trajectory tracking problem for a DWMR. This technique is used to design a kinematic controller that generates velocity control signals to compensate trajectory tracking errors providing robustness. These signals are set as the references for a dynamic controller that are designed by

means of an inverse dynamic control with a PD control to compensate the known forces and torques that actuate on the robot. As requirement this second controller must ensure a stable and fast tracking of the references spite of neglected dynamics to improve the robustness against chattering. The effectiveness in terms of robustness are evaluated by experimental results. It should be emphasized that the authors have already done some effort to achieve some solution [Elyoussef et al., 2010, 2012], but in those works the focus was just the kinematics and chattering analysis, and results were obtained by means of simulations.

In Section 2 the control problem is formulated. The design of controllers is presented in Section 3. Experimental results are presented in Section 4. Finally, in Section 5 conclusions and perspectives are discussed.

2. PROBLEM FORMULATION

2.1 Preliminaries

A typical example of a DWMR is depicted in Figure 1, which is an assembly of mechanical, electronic and electric systems. It comprises a body supported by four wheels, among which two are actuated by DC motors and the other two are free wheels, and also all the necessary devices to achieve autonomous motion, like drives, sensors and computer. Another important characteristic to be considered is the physical limitations, for example, in velocity, torque, sampling. Therefore, a precise model would be hard to develop and complex from the point of view of control design. Because of that a simple model that represent the main dynamics and kinematics of the DWMR, namely, the posture model, is extensively used in literature Yang and Kim [1999], Chwa [2004], Ferrara and Rubagotti [2008], Park et al. [2009]. An posture model with uncertainties was introduced by Park et al. [2009]:

$$\dot{\xi} = S(\xi)\,\eta \tag{1}$$

$$M_0(\xi)\dot{\eta} = -C_0(\xi,\dot{\xi})\,\eta + B_0(\xi)\,\tau - \psi(\xi,\eta) \tag{2}$$

in that the kinematics is represented in (1) and the dynamics in (2), for which: (i) $M_0(\xi)$ and $C_0(\xi,\dot{\xi})$ denote known smooth nominal functions; (ii) $\xi = [x\ y\ \theta]^T$ is the posture vector in the plane, with the robot localization, (x, y), and orientation, θ; (iii) $\eta = [v\ w]^T$ is the velocity vector, with longitudinal velocity, v, and rotational velocity, w; (iv) and $\tau = [\tau_r\ \tau_l]^T$ torque vector, with the torque in the right wheel, τ_r, and left wheel, τ_l (see Figure 1). The term $\psi(\xi,\eta)$ defined as

$$\psi(\xi,\eta) = \Delta M(\xi)\dot{\eta} + \Delta C(\xi,\dot{\xi})\,\eta + \tau_d \tag{3}$$

represents uncertainties associated to imperfect knowledge of physical parameters, unmodeled dynamics of actuators and sensors, and external disturbances. The Jacobian matrix are defined as:

$$S(\xi) = \begin{bmatrix} \cos(\theta) & 0 \\ \sin(\theta) & 0 \\ 0 & 1 \end{bmatrix}, \tag{4}$$

and the nominal inertial, Coriolis and input transformation matrices, respectively, $M(\xi)$, $C(\xi,\dot{\xi})$ and $B(\xi)$ are defined as in Elyoussef et al. [2012].

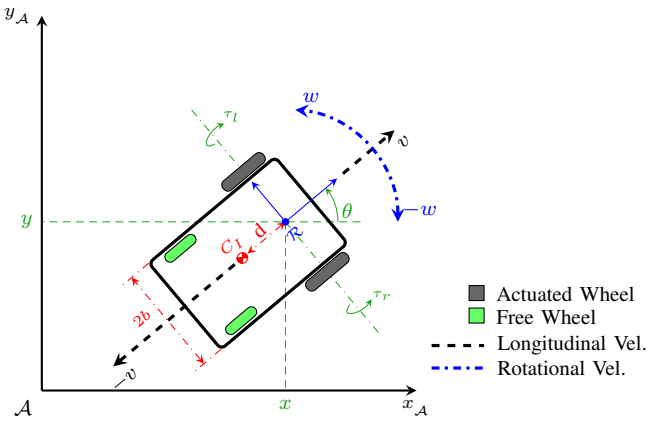

Fig. 1. DWMR representation and coordinate systems.

2.2 Problem Statement

Given the robot structure and assuming its posture and velocities known, the objective is to achieve a robust trajectory tracking control by means of SMC, that overcomes the lack of robustness provide by the commonly used FOSMC with BL [Yang and Kim, 1999, Chwa, 2004, Park et al., 2009] and avoids chattering.

Hence, the aim is accomplished by proposing a control structure that uses a SOSMC, the STSMC, for the design a robust kinematic controller and an inverse dynamic control with a PD for a dynamic controller design that achieves a stable fast velocity tracking, as depicted in Figure 2(a).

Definition 1. In this work, a geometrically feasible trajectory is that one the robot can execute by means of its basic movements, i.e the combination of longitudinal and rotational displacements in the case of the DWMR, and that the initial conditions are equal to the robot ones, or start in front of the robot for forward movements or behind the robot for backward movements, moreover, the initial orientation must generates errors smaller than $\pm\frac{\pi}{3}$.

3. CONTROL DESIGN

Let the control synthesis be treated separately by presenting first, the design of the dynamic control and then the design of the kinematic control.

3.1 Dynamic Control

The objective of the dynamic controller is to compensate the known torques and forces described in (2) and ensure fast tracking of the velocity error $\eta_e = \eta_c - \eta$ (see Figure 2(a)), therefore the uncertainties are set to zero for this design purpose and will be considered just for control gain adjust and the design of the kinematic controller. Now, let calculus of the inverse dynamic control be considered as presented by Spong et al. [2006], Elyoussef et al. [2012], that is:

$$\tau = B(\xi)^{-1}\left(C(\xi,\dot{\xi})\eta + M(\xi)\bar{u}\right), \tag{5}$$

which when applied to the system (2) results in:

$$\dot{\eta} = \bar{u}. \tag{6}$$

The vector $\bar{u} = [\bar{u}_v\ \bar{u}_w]^T$ is a new control input that will be designed as PD control to achieve fast convergence of η_e.

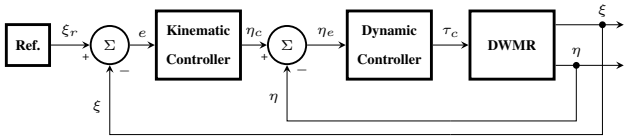

(a) Control structure.

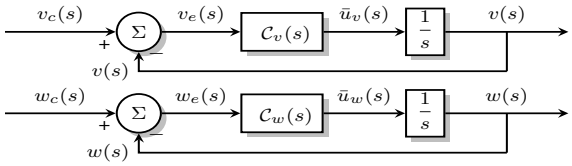

(b) Closed-loop diagram with the PD control.

Fig. 2. Control diagrams.

The desired control is detailed in Figure 2(b), in frequency domain. Thus, the control signal $\bar{u}_v(s)$ and $\bar{u}_w(s)$ are generated by the PD controllers:

$$\begin{aligned}\mathcal{C}_v(s) &= \frac{v(s)}{\bar{u}_v(s)} = k_{p_v} + \frac{k_{d_v}\, N_v}{1+\frac{N_v}{s}} \\ \mathcal{C}_w(s) &= \frac{w(s)}{\bar{u}_w(s)} = k_{p_w} + \frac{k_{d_w}\, N_v}{1+\frac{N_w}{s}},\end{aligned} \tag{7}$$

with the proportional gains, k_{p_v} and k_{p_w}, the derivative gains, k_{d_v} and k_{d_w}, and the derivative filter parameter gains N_v and N_w being positive and adjusted to achieve stability with good time response performance. The adjust of N_v and N_w plays an important role to accelerate the system response in spite of the neglected dynamics and avoid there excitation and the chattering phenomenon.

3.2 Kinematic Control

The kinematic control is developed using a strategy in that the DWMR is supposed to track a reference robot with the same kinematic behavior [Kanayama et al., 1990]:

$$\dot{\xi}_r = \; S_r(\xi_r)\eta_r \tag{8}$$

in that $\xi_r = [x_r \; y_r \; \theta_r]^T$ is the reference posture vector, $\eta_r = [v_r \; w_r]^T$ is the linear and angular reference velocities vector and the matrix $S_r(\xi_r)$ has the same structure as $S(\xi)$ in (4).

An error dynamics can be calculated as shown by Kanayama et al. [1990] as:

$$\dot{\xi}_e = f(\xi_e, \eta_c, \eta_r) = \begin{bmatrix} w_c\, y_e + v_r\, \cos(\theta_e) - v_c \\ -w_c\, x_e + v_r\, \sin(\theta_e) \\ w_r - w_c \end{bmatrix}, \tag{9}$$

for which the posture tracking error was defined as

$$\xi_e = \begin{bmatrix} x_e \\ y_e \\ \theta_e \end{bmatrix} = {}^{\mathcal{R}}R_{\mathcal{A}}(\theta)\,(\xi_r - \xi), \tag{10}$$

with the measurement of θ_e in the interval $-\pi \leq \theta_e \leq \pi$ and ${}^{\mathcal{R}}R_{\mathcal{A}}$ being the rotation matrix from $\mathcal{A}$ to $\mathcal{R}$.

Remark 1. The effect of the uncertainties and external disturbance that affect the system can be considered as a term $h(\xi,t) = [h_{x_e}(\xi,t) \;\; h_{y_e}(\xi,t) \;\; h_{\theta_e}(\xi,t)]^T$ added in the right-hand side of error dynamics, Equation (9). Now, recalling the invariance principle for SMC, described by Utkin et al. [2009], and assuming that the $h(\xi,t)$ is matched by control signal η_c, then one can conclude that if the system (9) is enforce to an sliding motion under some desired constraints, it will be ideally invariant to $h(\xi,t)$.

Based in Remark 1 and if it possible: (i) to find a sliding surface $\sigma(\xi_e) = 0$, with $\sigma(\xi_e) \in \Re^2$, that implies in a desired stable sliding motion for (9) and (ii) to design a switching control law:

$$\eta = \begin{cases} \psi_i^+(\xi_e) \text{ if } \sigma_i(\xi_e) > 0 \\ \psi_i^-(\xi_e) \text{ if } \sigma_i(\xi_e) < 0 \end{cases} \tag{11}$$

that enforces the system (9) to the manifold $\mathcal{M}(\xi_e) = \{\xi_e \in \Re^n : \sigma(\xi_e) = 0\}$, then the system (9) will be stable and ideally invariant to matched uncertainties and external disturbances.

Unfortunately, in practical implementation there are neglected dynamics and sampling frequency limitation that causes the chattering phenomenon. The commonly used FOSMC with BL can avoid chattering but robustness degree decrease substantially in some cases.

Hence, the STSMC, a SOSMC where a continuous control signal with discontinuous derivative is used to enforce a sliding motion second order in the manifold $\mathcal{S}(.) = \{x \in \Re^n : \sigma(.) = \dot{\sigma}(.) = 0\}$ is better choice to design the kinematic controller, because it ensures better effectiveness in terms of robustness against parameter and structural uncertainties and sampling frequency limitation [Levant, 1993, Fridman and Levant, 2002, Ferrara and Rubagotti, 2008].

Let the kinematic control design starts considering error dynamics (9) to define constraints in vector of surfaces form with the same control input dimension that implies in a stable sliding motion with good performance. It should be emphasized that uncertainties are not part of this first design step and are considered later. Therefore, a sliding surface $\sigma(\xi_e) = [\sigma_v(\xi_e) \; \sigma_w(\xi_e)]^T = 0$, with $\sigma_v(\xi_e)$ related to v_c and $\sigma_w(\xi_e)$ to w_c, must be designed to constraint the state trajectories of (9) to a stable sliding motion. Using an iterative process of choosing restrictions and evaluating the resulting sliding mode dynamics, by means of the equivalent control method [Utkin et al., 2009], the selection of the sliding surfaces have been refined to:

$$\sigma(\xi_e) = \begin{bmatrix} \sigma_v(x_e) \\ \sigma_w(y_e, \theta_e) \end{bmatrix} = \begin{bmatrix} k_1 x_e \\ k_2 y_e + k_3\, \sin(\frac{\theta_e}{2}) \end{bmatrix} = 0, \tag{12}$$

with k_1, k_2 and k_3 being control parameters. The component $\sigma_v(x_e)$ was chosen only as function of x_e because it is associated with v_c, which acts only in the dynamics of x_e. Therefore, y_e and θ_e were left to be treated by the component $\sigma_w(y_e, \theta_e)$. The sinusoidal term $\sin(\frac{\theta_e}{2})$ was necessary to achieve a desired stable sliding mode dynamics as demonstrated in sequence. Moreover, the ratio $\frac{\theta_e}{2}$ ensures that $\sin(\frac{\theta_e}{2})$ is equal zero just for $\theta_e = 0$ in the interval of interest $-\pi \leq \theta_e \leq \pi$.

Theorem 1. By choosing the sliding surfaces (12) to the error dynamics (9) and considering $\eta = \eta_c$ (fast velocity tracking and uncertainties compensation), the following sliding mode dynamics is obtained:

$$\dot{\theta}_e = -\frac{2\,k_2\,\sin(\theta_e)v_r}{k_3\cos(\frac{\theta_e}{2})}. \tag{13}$$

Proof. The equivalent control $\eta_{eq} = [v_{eq}\ w_{eq}]^T$, which satisfies the condition $\dot{\sigma} = \dfrac{\partial\sigma(\xi_e)}{\partial\xi_e}\cdot f(\xi_e,\eta_c,\eta_r) = 0$ [Utkin et al., 2009], is calculated as:

$$\begin{aligned} v_{eq} =& w_{eq}\,y_e + \cos(\theta_e)v_r \\ w_{eq} =& \frac{1}{2}\frac{k_3\,\cos(\frac{\theta_e}{2})\,w_r + 2\,k_2\,\sin(\theta_e)\,v_r}{\mathcal{G}_w(x_e,\theta_e)}, \end{aligned} \tag{14}$$

with:

$$\mathcal{G}_w(x_e,\theta_e) = k_2\,x_e + \frac{k_3}{2}\,\cos(\frac{\theta_e}{2}). \tag{15}$$

The sliding mode dynamics (13) is determined by substituting the equivalent control (14) in (9) and simplifying by taking into account that $\sigma = \dot{\sigma} = 0$ in sliding mode.

Theorem 2. Given the measurement of θ_e in the interval $-\pi \le \theta_e \le \pi$ and the adjust $k_3 > 0$ then: if $v_r > 0$ the system (13) is asymptotically stable for $k_2 > 0$; and if $v_r < 0$ the system (13) is asymptotically stable for $k_2 < 0$.

Proof. Consider the Lyapunov function:

$$V_{sm}(\theta_e) = \frac{1}{2}\theta_e^2, \tag{16}$$

which time derivative is calculated as:

$$\dot{V}_{sm}(\theta_e) = -\frac{2\,k_2\,\theta_e\,\sin(\theta_e)\,v_r}{k_3\cos(\frac{\theta_e}{2})}. \tag{17}$$

Note that $\dot{V}_{sm}(\theta_e)$ is negative if the sign of k_2 and v_r are equal for $-\pi \le \theta_e \le \pi$ except for $\theta_e = 0$, in which $V_{sm}(0) = 0$.

Corollary 3. The values of $\dot{\theta}_e$ and $\dot{V}_{sm}(\theta_e)$ in $\theta_e = \pm\pi$ can be calculated using the L'Hospital's rule as:

$$\lim_{\theta_e\to\pm\pi}\dot{\theta}_e = \mp\frac{4\,k_2}{k_3}v_r. \tag{18}$$

$$\lim_{\theta_e\to\pm\pi}\dot{V}_{sm}(\theta_e) = \mp\frac{4\,\pi\,k_2}{k_3}v_r. \tag{19}$$

Remark 2. Measuring θ_e in the interval $-\pi \le \theta_e \le \pi$ implies that $0 \le \cos(\dfrac{\theta_e}{2}) \le 1$, and taking to account the adjust of k_2 described in Theorem 2, the Definition 1 and the posture error definition (10), that imply that x_e is positive for forward movements and negative for backward movements, then $\mathcal{G}_w(x_e,\theta_e) > 0$ for a SMC for which the switching variable $\sigma_v(x_e)$ is driven monotonically to zero.

Remark 3. The sliding motion clearly does not depend on k_1, however, for simplicity it is assumed that $k_1 > 0$. On other hand, the convergence of this dynamics can be adjusted by the ratio $\dfrac{k_2}{k_3}$, that should adjusted ensure good convergence and avoid unnecessary control effort.

Now, let the control signal η_c be design by means of STSMC algorithm presented by Levant [1993], Fridman and Levant [2002] to achieve a second order sliding motion in the manifold $\mathcal{S}(\xi_e) = \{\xi_e \in \Re^3 : \sigma(\xi_e) = \dot{\sigma}(\xi_e) = 0\}$, for $\sigma(\xi_e) = 0$ defined in (12). In this step, the uncertainties represented by $h(\xi_e,t)$ are considered to formulate an auxiliary control system defined by the variables $y_1 = \sigma(x_e)$, $y_2 = \dot{\sigma}(x_e)$, $z_1 = \sigma(y_e,\theta_e)$ and $z_2 = \dot{\sigma}(y_e,\theta_e)$:

$$\begin{aligned} \dot{y}_1 &= y_2 \\ \dot{y}_2 &= \mathcal{F}_v(x_e,y_e,\theta_e,v_r,w_r,w_c,\dot{w}_c) - \mathcal{G}_v\dot{v}_c \end{aligned} \tag{20}$$

with:

$$\begin{aligned} \mathcal{F}_v(\cdot) =& k_1\,\dot{w}_c\,y_e - k_1\,w_c^2\,x_e - k_1\,\sin(\theta_e)v_r\,w_r \\ &+ 2\,k_1\,\sin(\theta_e)\,v_r\,w_c + k_1\cos(\theta_e)\dot{v}_r + k_1\frac{d}{dt}h_{x_e}(\xi,t) \\ \mathcal{G}_v =& k_1, \end{aligned} \tag{21}$$

and:

$$\begin{aligned} \dot{z}_1 &= z_2 \\ \dot{z}_2 &= \mathcal{F}_w(y_e,\theta_e,v_r,w_r,v_c,w_c) - \mathcal{G}_w(x_e,\theta_e)\dot{w}_c, \end{aligned} \tag{22}$$

with:

$$\begin{aligned} \mathcal{F}_w(\cdot) =& -\frac{k_3}{4}\left(\sin(\frac{\theta_e}{2})(w_r - w_c)^2 - 2\,\cos(\frac{\theta_e}{2})\,\dot{w}_r\right) \\ &-k_2\,\left(w_c^2\,y_e + v_r\cos(\theta_e)\,(2\,w_c - w_r) - \sin(\theta_e)\,\dot{v}_r\right. \\ &\left.-v_c\,w_c\right) + k_2\frac{d}{dt}h_{y_e}(\xi,t) + \frac{k_3}{2}\frac{d}{dt}\left(\cos(\frac{\theta_e}{2})h_{\theta_e(\xi,t)}\right) \\ \mathcal{G}_w(x_e,\,\theta_e) =& k_2\,x_e + \frac{k_3}{2}\cos(\theta_e). \end{aligned} \tag{23}$$

Given that there are the following limits:

$$\begin{aligned} &\|\mathcal{F}_v(\cdot)\| \le C_v, \quad \|\mathcal{G}_v(\cdot)\| = k_1 > 0, \\ &\|\mathcal{F}_w(\cdot)\| \le C_w, \quad 0 < \Psi_m \le \|\mathcal{G}_w(\cdot)\| \le \Psi_M, \end{aligned} \tag{24}$$

then the following STSMC algorithm:

$$\begin{aligned} v_c &= v_1 + v_2 & w_c &= w_1 + w_2 \\ v_1 &= a_v\sqrt{\|y_1\|}\mathrm{sign}(y_1) & w_1 &= a_w\sqrt{\|z_1\|}\mathrm{sign}(z_1) \\ \dot{v}_2 &= b_v\,\mathrm{sign}(y_1) & \dot{w}_2 &= b_w\,\mathrm{sign}(z_1) \end{aligned} \tag{25}$$

with the gain adjust:

$$\begin{aligned} a_v^2 &\ge \frac{4C_v}{k_1^2}\frac{(b_v + C_v)}{(b_v - C_v)}, \quad b_v \ge \frac{C_v}{k_1} \\ a_w^2 &\ge \frac{4C_w}{\Psi_m^2}\frac{\Psi_M(b_w + C_w)}{\Psi_m(b_w - C_w)}, \quad b_w \ge \frac{C_w}{\Psi_m}, \end{aligned} \tag{26}$$

ensures finite time convergence for the systems (20) and (22). The convergence proof can be found in the work of Levant [1993], that stability conditions were refined by Fridman and Levant [2002]. Therefore the desired sliding motion is guaranteed achieving the robust tracking control for the DWMR.

Remark 4. The conditions (24) are reasonable under the delimitation of the feasible trajectories, Definition 1 and the existence of operating limitations. Note also that the limits for $\mathcal{G}_w(x_e,\theta_e)$ (24) agree with Remark 2.

4. RESULTS

4.1 Preliminaries

In this section, some experimental results and analysis are presented to demonstrated the performance and robustness of the proposed strategy. The kinematic controller based on a FOSMC with BL [Elyoussef et al., 2012]:

Fig. 3. Powerbot

$$v_c = \rho_v \frac{y_1}{\|y_1\| + \epsilon_v}$$
$$w_c = \rho_w \frac{y_2}{\|y_2\| + \epsilon_w} \quad (27)$$

is considered for comparative study with proposed one.

The study are concentrated in the analysis of the linear distance error signal between reference and actual posture, $e(x_e, y_e) = \sqrt{x_e^2 + y_e^2}$, and angular error signal, θ_e, and their RMS values performed by the robot, when it is tracking circular trajectories, which are commonly in the literature [Yang and Kim, 1999, Chwa, 2004, Park et al., 2009]. Two different trajectories are used, namely: (i) C1 with $v_r = 0.5$ m/s and $w_r = \frac{\pi}{10}$ rad/s, (ii) C2 with $v_r = 1$ m/s and $w_r = \frac{\pi}{5}$ rad/s.

The platform Powerbot depicted in Figure 3 is considered for the tests. This DWMR have mass $m = 120$ kg, dimensions $0.90 \times 0.66 \times 0.48$ m and two wheels actuated by two DC motors with maximum torque of 20.45 N.m. Its load capacity is 100 kg and its input variables are the longitudinal velocity v_c, with a maximum value of 2.1m/s, and the rotational velocity w_c, with a maximum value of 5.24 rad/s. Unfortunately, the platform is closed and there are internal PID controllers that tracks these inputs with a sampling time of 5ms. Thus, only the PD controller can be considered as dynamic controller for the implementation. Actually, this displeased situation is commonly found in the literature of robotics as in Yang and Kim [1999], Spong et al. [2006]. The kinematic controllers (STSMC and FOSMC with BL) are implemented in an application running on the embedded computer that operates with sampling of 15ms.

4.2 Experiments

In this section the experimental results in that Powerbot is required to track the trajectories C1 and C2 are explored. The gains of PD controllers are adjusted as $k_{p_v} = 40$, $k_{p_w} = 40$, $k_{d_v} = 20$ and $k_{d_w} = 20$ as indicated by the factory. Although, it is not possible implement compensation of the dynamics, sufficient analysis results are obtained studying two different control structures comprising the embedded PD controllers in cascade with the kinematic controller based on: (i) the FOSMC with BL (27), (ii) and the STSMC (25). For both controllers the surface gains were adjusted as $k_1 = 1$, $k_2 = 5$ and $k_3 = 2$ considering Remark 3.

The results for the control structure with the FOSMC with BL were obtained considering the controller parameters (27) being adjusted as $\rho_v = \rho_w = 1$ and $\epsilon_v = \epsilon_w = 0.1$. Substantial values of $\epsilon_v = \epsilon_w$ to enlarge the BL and reduced control effort were necessary to enforce a sliding mode. Performing trajectory C1, the error signals $e(x_e, y_e)$ and θ_e (see Figures 4(a) and 4(b)), converged, respectively, to values around 10 cm and 7×10^{-2} rad, which are reasonable.

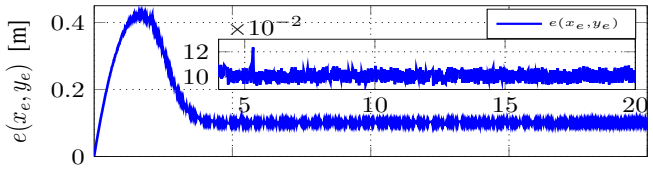

(a) Error $e(x_e, y_e)$

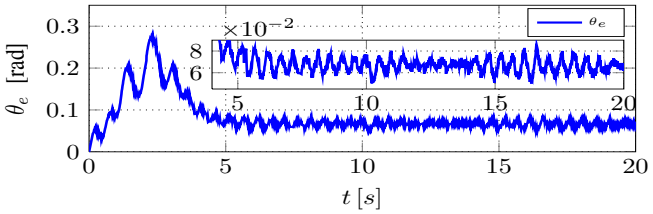

(b) Error θ_e

Fig. 4. Experimental results for the control strategy using the FOSMC with BL - Trajectory C1.

On the other hand, the error signals $e(x_e, y_e)$ and θ_e obtained with trajectory C2, depicted in Figures 5(a) and 5(b), converged, respectively, to values around 65 cm and 0.45 rad, which are not good taking into account the dimensions of Powerbot. The gains readjustment were not successful due to system limitations.

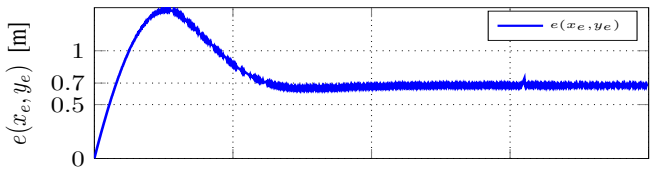

(a) Error $e(x_e, y_e)$

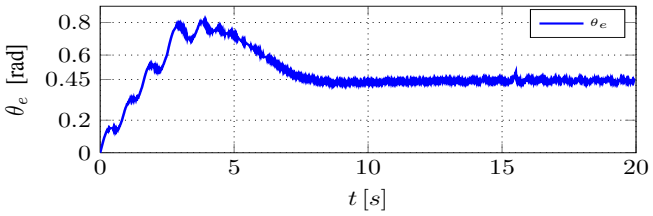

(b) Error θ_e

Fig. 5. Experimental results for the control strategy using the FOSMC with BL - Trajectory C2.

Now let the results for the STSMC control structure be considered. The control gains were adjusted as $a_v = 0.7$, $b_v = 0.1$, $a_w = 0.5$ and $b_v = 0.1$ to ensure sliding motion and good performance. The first test with trajectory C1 resulted in the errors signals $e(x_e, y_e)$ and θ_e depicted in Figures 6(a) and 6(b), which converged to values around 5 mm and 5×10^{-3} rad, hence smaller than that obtained using the FOSMC with BL.

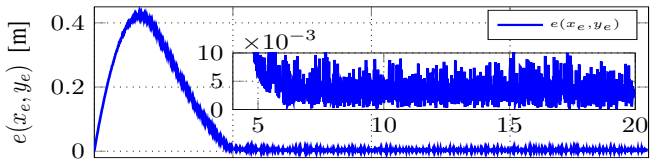

(a) Error $e(x_e, y_e)$

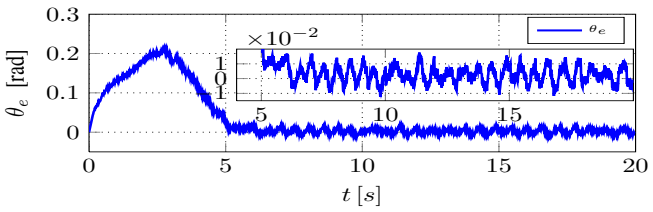

(b) Error θ_e

Fig. 6. Experimental results for the control strategy using the STSMC - Trajectory C1.

Differently from the case where the FOSMC with BL failed to track the trajectory C2, using STSMC, the errors signals $e(x_e, y_e)$ and θ_e converged to values around 1 cm and 1×10^{-3} rad as depicted in Figures 7(a) and 7(b), which is a satisfactory result in terms of robustness.

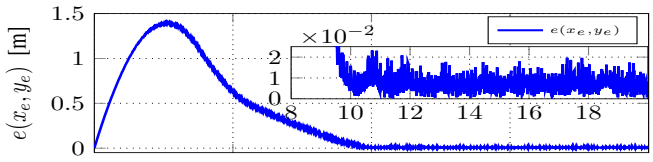

(a) Error $e(x_e, y_e)$

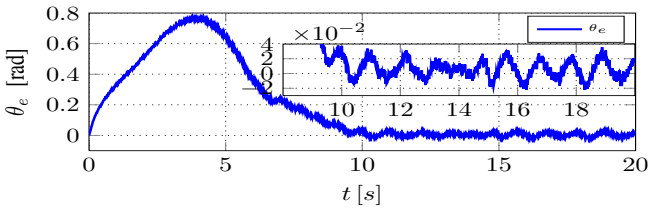

(b) Error θ_e

Fig. 7. Experimental results for the control strategy using the STSMC - Trajectory C2.

In Table 1 the results obtained with the experiments are summarized with the RMS values of $e(x_e, y_e)$ and θ_e. In all situations structure with the STSMC has smaller errors, showing more effectiveness in terms of robustness.

Table 1. RMSE (Root Mean Square Error) of the trajectory tracking errors from the experimental results.

Trajectory	Variable	SMC with BL	STSMC
C1	$e(x_e, y_e)$	0.1010	4.1×10^{-3}
	θ_e	0.0668	6.1×10^{-3}
C2	$e(x_e, y_e)$	0.6785	8.8×10^{-3}
	θ_e	0.4426	1.31×10^{-2}

5. CONCLUSIONS AND PERSPECTIVES

In this work, a control structure comprising a dynamic controller, designed with the inverse dynamic control technique and the PD control technique, in cascade with a kinematic controller, designed with a SOSMC, namely, STSMC, were successfully proposed as a robust solution for the trajectory tracking control problem for a *nonholonomic* mobile robot by means of a SMC. The results were demonstrated with experimental analysis.

The main future work is to extend the PD-super-twisting second order sliding mode tracking control for a class of nonholonomic underactuated systems. An stability analysis based singular perturbation theory of the whole control loop is another objective to refined stability conditions. As well as, considering dynamic limitations to generate feasible trajectories to achieve better performance. Finally, there is scheduled some hardware updated for Powerbot, to allow the implementation the inverse dynamic control.

REFERENCES

Dongkyoung Chwa. Sliding-mode tracking control of nonholonomic wheeled mobile robots in polar coordinates. *Control Systems Technology, IEEE Transactions on*, 12 (4):637–644, 2004.

Ebrahim Samer Elyoussef, Nardênio Almeida Martins, Douglas Wildgrube Bertol, Edson Roberto De Pieri, and Marc Jungers. On a Wheeled Mobile Robot Tracking Control: Sliding Mode Control Design. In *XVII Congresso Brasileiro de Automática*, September 2010.

Ebrahim Samer Elyoussef, Edson Roberto De Pieri, Ubirajara Franco Moreno, and Marc Jungers. Super-twisting sliding modes tracking control of a nonholonomic wheeled mobile robot. In *10th International IFAC Symposium on Robot Control, SYROCO'12*, 2012.

Antonella Ferrara and M. Rubagotti. Second-order sliding-mode control of a mobile robot based on a harmonic potential field. *IET Control Theory and Applications*, 2 (9):807–818, March 2008.

L. Fridman and A. Levant. Higher order sliding modes. *Sliding mode control in engineering*, 11:53–102, 2002.

Y. Kanayama, Y. Kimura, F. Miyazaki, and T. Noguchi. A stable tracking control method for an autonomous mobile robot. In *Robotics and Automation, 1990. Proceedings., 1990 IEEE International Conference on*, pages 384–389 vol.1, 1990.

Arie Levant. Sliding order and Sliding accurancy in sliding mode control. *Int. Journal of Control*, 58(6):1247–1263, 1993.

Bong Seok Park, Sung Jin Yoo, Jin-Bae Park, and Yoon-Ho Choi. Adaptive neural sliding mode control of nonholonomic wheeled mobile robots with model uncertainty. *Control Systems Technology, IEEE Transactions on*, 17(1):207–214, 2009.

Bruno Siciliano and Oussama Khatib. *Handbook of Robotics*. Springer, 2008. ISBN 978-3-540-23957-4.

Mark W. Spong, Seth Hutchinson, and M. Vidyasagar. *Robot Modeling and Control*. John Wiley & Sons, 1 edition, 2006. ISBN 0-471-64990-2.

Vadim I. Utkin, Jürgen Guldner, and Jingxin Shi. *Sliding Mode Control in Electro-Mechanical Systems*. CRC Press, second edition, 2009. ISBN 13:978-1-4200-6560-2.

Jung-Min Yang and Jong-Hwan Kim. Sliding mode control for trajectory tracking of nonholonomic wheeled mobile robots. *Robotics and Automation, IEEE Transactions on*, 15(3):578–587, 1999.